RESEARCH ARTICLE

Design of improved ZigBee routing algorithm for the application of farmland information data acquisition and analysis

Ping Liu[1, *] and Hui Zhu[2]

[1]Department of Information Engineering, [2]Public Infrastructure Department, Ganzhou Polytechnic, Ganzhou, Jiangxi, China.

Received: January 17, 2024; **accepted:** March 8, 2024.

Efficient modern agricultural production relies on accurate farmland data. However, manual recording, the current method of data collection, is inefficient and prone to errors. This study aimed to improve the efficiency and accuracy of farmland data collection. The study addressed the problem of accurately and conveniently collecting farmland information data in complex environments and effectively analyzing it. A new solution was proposed, which utilized improved ZigBee network technology for both data collection and analysis *via* the newly introduced Improved ZigBee Routing (IMP-ZBR) protocol. The protocol enhanced the intermediate node forwarding mechanism, updated routing rules, and optimized caching paths. These improvements led to reduced energy consumption by the nodes and increased network capacity. To enhance the management of data collected from various sensors, a heterogeneous data fusion method based on cloud modeling and an improved evidence theory design were also proposed in this study. This method offered a more precise depiction of data uncertainty. The results showed that the IMP-ZBR protocol enhanced packet delivery rates by an average of 4.5%, diminished route discovery frequency by 14%, reduced average delay by 44 ms, and lowered route control overhead by 12% for different Constant Bit Rate (CBR) packet origination speeds. The heterogeneous data fusion technique proposed concentrated with high assurance. As a result of the comprehensive study, the proposed system demonstrated significant advantages in reducing network congestion and enhancing system performance. Moreover, it could offer substantial assistance for agricultural modernization.

Keywords: ZigBee technology; smart agriculture; information acquisition; data transmission; heterogeneous data fusion.

[*]**Corresponding author:** Ping Liu, Department of Information Engineering, Ganzhou Polytechnic, Ganzhou 341000, Jiangxi, China. Emails: LP18970716909@163.com.

Introduction

As the global population continues to grow, the demand for food production increases [1, 2]. For many countries, expanding arable land is not a viable option. Therefore, precision agriculture is a more suitable approach to improve unit land output. The essence of precision agriculture is in the precise and efficient gathering of farmland data, which is also necessary for analyzing crop growth and implementing agricultural interventions [3, 4]. Currently, most precision agriculture industries still rely on primitive human methods to collect farmland data. This approach has several issues, including low collection efficiency and difficulty in ensuring data quality [5]. Therefore, it is necessary and urgent to adopt automation and computer technology for automatic farmland data collection. ZigBee technology, a wireless local area network protocol based on the IEEE 802.15.4 specification, can be a viable solution.

Due to its advantages of low power consumption, low cost, support for large-scale networks, low network latency, and reliability, it is increasingly being applied in modern agriculture and other fields [6, 7]. Nowadays, ZigBee wireless network technology is rapidly developing and gaining attention in many fields. Researchers both domestically and internationally have done a lot of studies on it, especially in routing protocols. Gao *et al*. proposed node-protection-based Zigbee routing (NPZBR) algorithm. In comparison to the conventional Zigbee routing algorithm, the experimental findings demonstrated that the suggested method decreased end-to-end delay and node mortality while increasing node survival rate by 4% and reducing energy usage by 10% [8]. Heidari *et al*. proposed and simulated a routing protocol based on whale optimization algorithm. The protocol performed clustering by considering factors. According to the findings, the suggested strategy performed noticeably better than alternative approaches in terms of the quantity of dead nodes [9]. Gao *et al*. introduced RowBee, a routing system based on CTC technology. RowBee allowed nodes to choose their duty cycle and employed Wi-Fi nodes to assist ZigBee nodes in creating routing patterns. Simultaneously, a straightforward yet efficient technique was implemented to enable ZigBee nodes to awaken simultaneously with the beacons transmitted by Wi-Fi nodes. RowBee could considerably lower the end-to-end delay, according to experimental results [10]. Bodunde *et al*. presented the architectural design and performance evaluation of an adaptive sprinkler robot that was interfaced through ZigBee communication to improve the efficiency of the prototype. The results summarized the performance of the system in terms of the amount of water carried, the distance irrigated per cycle, and the time required to irrigate a given area of farmland [11]. Chi *et al*. introduced a novel cross-layer design called Amphista, which used meticulous channel state information from Wi-Fi to parse simultaneously transmitted ZigBee to Wi-Fi messages, a unique feature that made it possible to forward both uplink and downlink data in a single ZigBee data stream. Experimental results revealed that Amphista significantly improved throughput up to 400 times and reduced latency [12].

The agricultural information monitoring system can provide important information such as crops and soil data for managers. The collected data can serve as a basis for decision-making in intelligent agriculture. Pilger *et al*. developed a program for acquiring remote sensing images of agricultural land. The results indicated that the agricultural remote sensing images obtained through this method had lower noise levels compared to traditional methods with a consistency rate of over 93% [13]. Lin *et al*. proposed a hierarchical data collection scheme for unmanned aerial vehicle-assisted industrial wireless sensor networks. The scheme was particularly suitable for agricultural monitoring applications that required image data collection. It used a combination of precise and greedy methods for compressed sampling and improved the linear programming formula by using the precise modeling method of the energy optimal formula. The balance factor parameters were constructed using the greedy method. According to the experimental results on agricultural image data collection, this scheme could cluster nodes adaptively in different layers and scheduled drones for energy-saving data collection, which effectively improved the efficiency of drone data collection [14]. Stoll *et al*. discovered that, while independent Controller Area Network (CAN) data recorders were a convenient way to collect performance data for agricultural machinery equipment, this method could only capture data from interpretable messages broadcasted through the mechanical CAN bus. For mechanical performance parameters that could not be explained through CAN data, other methods were necessary to record these variables. The researchers had designed a solution that included electronic controller units and allowed CAN data recorders to transmit data through fractor. The results demonstrated that the solution could effectively collect interpretable messages broadcasted by the mechanical CAN bus in agricultural machinery equipment [15]. A novel multi-sensor data fusion technique was proposed by Xiao, based on a new trust entropy and difference in evidence measure. The researcher measured the amount of information in the evidence using belief entropy to represent the relative importance of the evidence and modified the trustworthiness of each evidence into a weight based on its information [16]. Lin *et al.*, in light of the widespread use of smart flowmeters, investigated the information security of flowmeter communication networks based on multi-sensor data fusion and artificial intelligence-driven flowmeter information security. The outcomes of the experiment demonstrated that the generalized flowmeter intelligent processing system with its benefits including high resource utilization, a single standard, and a broad application range had a lot of room for growth in the future [17].

Despite extensive research has been done from various countries to enhance the effectiveness of the ZigBee routing algorithm, there is still a lack of research on designing data collection models based on the algorithm to meet the needs of agricultural data collection work. As an emerging wireless network technology, ZigBee wireless network technology is characterized by short communication distance and low power consumption. The technology contains a set of special communication specifications that can support long-distance information transfer [18]. Due to the use of mechanized management and data collection systems in agricultural areas, ZigBee wireless network technology is suitable for long-distance data transmission. Additionally, in farmland, crops are widely distributed, and there may be many monitoring points. ZigBee wireless network technology enables automatic networking, making it beneficial for large-scale data collection in farmland areas. ZigBee wireless network technology is better suited for constructing data collection systems in agricultural areas. This research aimed to fully utilize the advantages of the ZigBee routing algorithm in the field of farmland data collection (DC) based on ZigBee technology and used a tree network topology to construct a DC and analysis system for farmland information. The result of this study would provide assistance for the development of smart agriculture.

Materials and methods

Design of improved ZigBee routing (IMP-ZBR) protocol for farmland information data collection system

The structure of ZigBee-based wireless sensing network was shown in Figure 1. ZigBee network mainly contained coordinator (sensor) nodes, routing nodes, and inductor nodes. For the coordinator node, it collected the farmland data at regular intervals and then transmitted it to the coordinator node step by step with the help of routing node. The coordinator node could support the formation of the network and allow the joining of nodes. It could also transfer the farmland data obtained by the routing nodes or sensor nodes to the personal computer (PC) through general packet radio service (GPRS) network and store the data in a specific database to complete the collection, transferring, and storage of farmland data. Routing nodes, on the other hand, were primarily responsible for forwarding information as well as maintaining paths within the network and could also act as a parent device to support the entry of sensors into the network. Sensor nodes combined DC, transmission, and processing modules in a smaller physical unit that could support DC and ensure communication between nodes. It was important to note that, due to the nature of ZigBee itself and the application requirements of the DC project, the system design needed to take into account some of the key technical issues involved in the project, such as the low power consumption design and the data fusion technology for the wireless sensor network. Considering ZigBee's agricultural wireless sensor network, the IMP-ZBR protocol was designed. The IMP-ZBR protocol was based on the ZigBee routing algorithm and could be used for various functions in wireless communication networks, including route discovery, route maintenance, data transmission, communication path

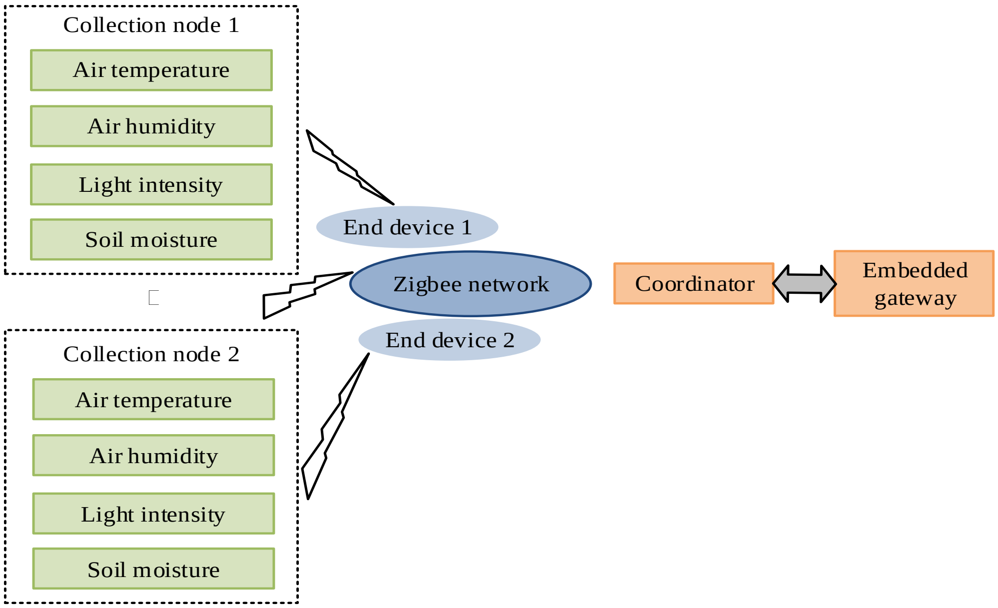

Figure 1. Schematic of a ZigBee-based wireless sensor network architecture.

optimization, and self-organization. The IMP-ZBR protocol differed from the ZigBee routing algorithm in that it aimed to balance energy loss and load, while the latter employed a node state classification method and a routing update criterion based on node energy consumption. Since batteries are typically used to power nodes in ZigBee networks, the routing protocol must account for the nodes' energy consumption. Particularly in the context of agricultural internet of things (IoT), an increase in sensors will result in an increase in the amount of data that needs to be processed in each node's cache queue and an acceleration of the nodes' energy consumption, which will shorten the network's life cycle and possibly cause network congestion. To address these issues, a routing protocol IMP-ZBR had been designed with the goal of reducing energy loss and load balancing. Specifically, the Queue Cache Packet Occupancy Ratio Q_{cr} , which was defined as the maximum queue length $L_{cq\max}$ and the queue length L_{cq} in the node as specified by the protocol, were used by the IMP-ZBR algorithm to determine the load of the node, which was accomplished by introducing a cross-layer strategy to obtain information about queue cache packets from the MAC layer. Simultaneously, the node's energy consumption was determined by calculating the energy consumption occupancy ratio E_{cr} using the node's consumed energy and total energy E_{int} , as indicated by equation (1).

$$\begin{cases} Q_{cr} = L_{cq} / L_{cq\max} \\ E_{cr} = \left(E_{\text{int}} - E_{left}\right) / E_{\text{int}} \end{cases} \tag{1}$$

where E_{left} was the energy remaining in the node after working for some time. IMP-ZBR also designed a node state partitioning method. The congestion state was divided into three levels as idle, general, and congested with the boundaries of $Q_{cr} = 50\%$ and $Q_{cr} = 80\%$, and the labels of 0, 1, and 2, respectively. The energy of network nodes was divided into three levels as sufficient, general, and insufficient with the boundaries of $E_{cr} = 50\%$ and $E_{cr} = 80\%$, and the labels of 0, 1, and 2, respectively. After considering the different states of the node, it decided whether the node was suitable as an intermediate node to participate in the establishment of the path. The forwarding strategy of the intermediate node was shown in Figure 2.

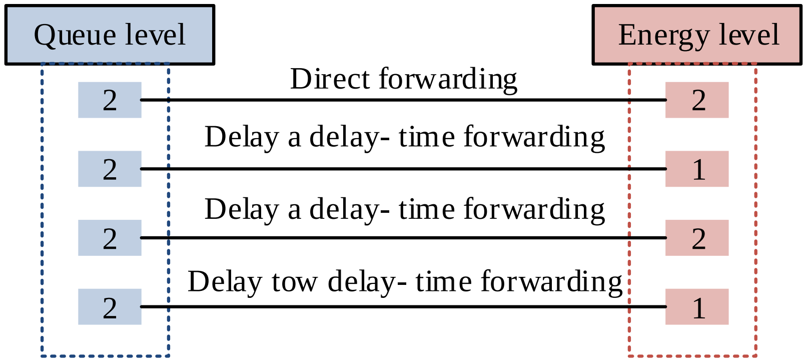

Figure 2. Forwarding strategy of intermediate node.

The IMP-ZBR algorithm also designed a routing update criterion for the ZigBee routing protocol. The IMP-ZBR protocol adopted a new route update criterion, i.e., *Cost* value. The *Cost* value was computed based on the sum of node's energy consumption ratios, sum of node's load ratios, and the sum of link qualities, which was calculated as shown in equation (2).

$$Cost = \left(\alpha \sum Q_{cr} + \beta \sum E_{cr} + \lambda \frac{1}{\sum LQI} \right) / hop\_count \quad (2)$$

where hop_count was the total number of hops. α , β , and λ were the weight values and $\alpha + \beta + \lambda = 1$. LQI was the value of link quality in the node, which was calculated as shown in equation (3).

$$LQI = 255(81 - RSSI)/91 \quad (3)$$

where RSSI information was contained in the data packets and could be read by the structure metrics. In the traditional ZigBee routing protocol, once the data transmission path is broken, it is handled in a more limited way and the network nodes are involved in data transmission and route construction more frequently, which leads to an increase in the network routing load. Therefore, the IMP-ZBR algorithm optimized the route construction method.

The flow of the path caching strategy was shown in Figure 3. The destination node initiated the cache timer upon receiving the RREQ packet and responded to the source node with the RREP packet in accordance with the arrival order. Following receipt of the initial RREP packet, the source node would cache all incoming RREP packets until the timer expired, prioritizing the packets based on a predetermined scale to determine the optimal path. Additionally, during the route establishment process, this path caching strategy compared the combined performance index *Cost* value of each feasible route, choosing the path with the smallest *Cost* value as the primary path for data transmission. This process determined which path had the lowest A value, which avoided consuming excessive network resources in maintaining multiple alternate paths, and thus selected an optimal alternate path.

The flow of the IMP-ZBR protocol for handling RREQ was shown in Figure 4. After the RREQ packet arrived at a node, that node first determined whether the RREQ packet was sent by itself or not. If it was, then the RREQ packet was directly discarded, otherwise it checked whether there was a reverse routing table in that node that could reach the source node. If the routing criterion of RREQ packet of the source node was less than the update criterion cost value of the reverse route, then the reverse routing table was updated, otherwise it operated according to the intermediate node forwarding policy and enforced the path caching policy for the destination node.

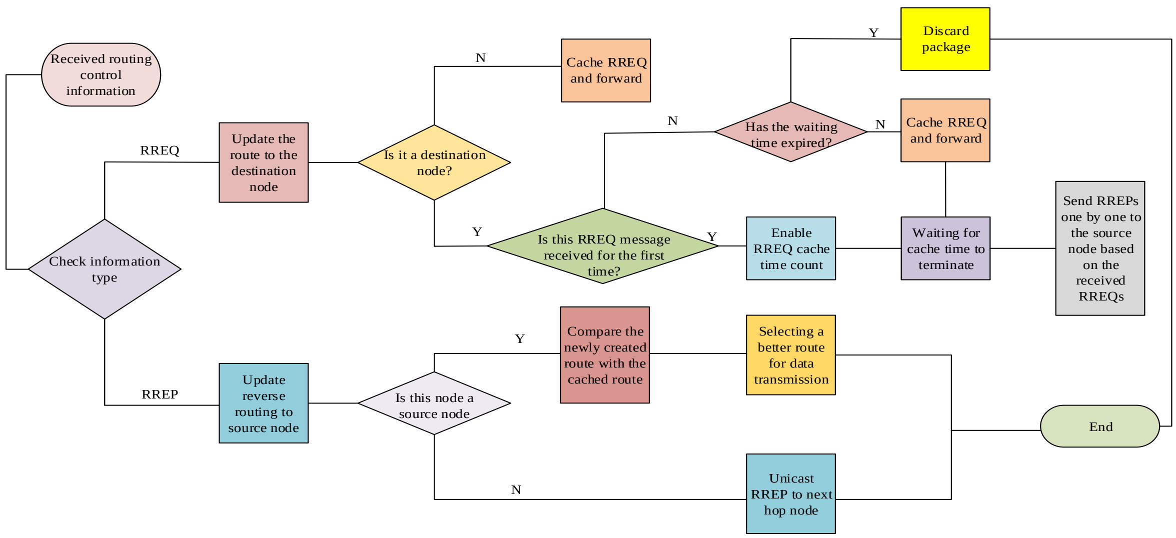

Figure 3. The flow of the path caching strategy.

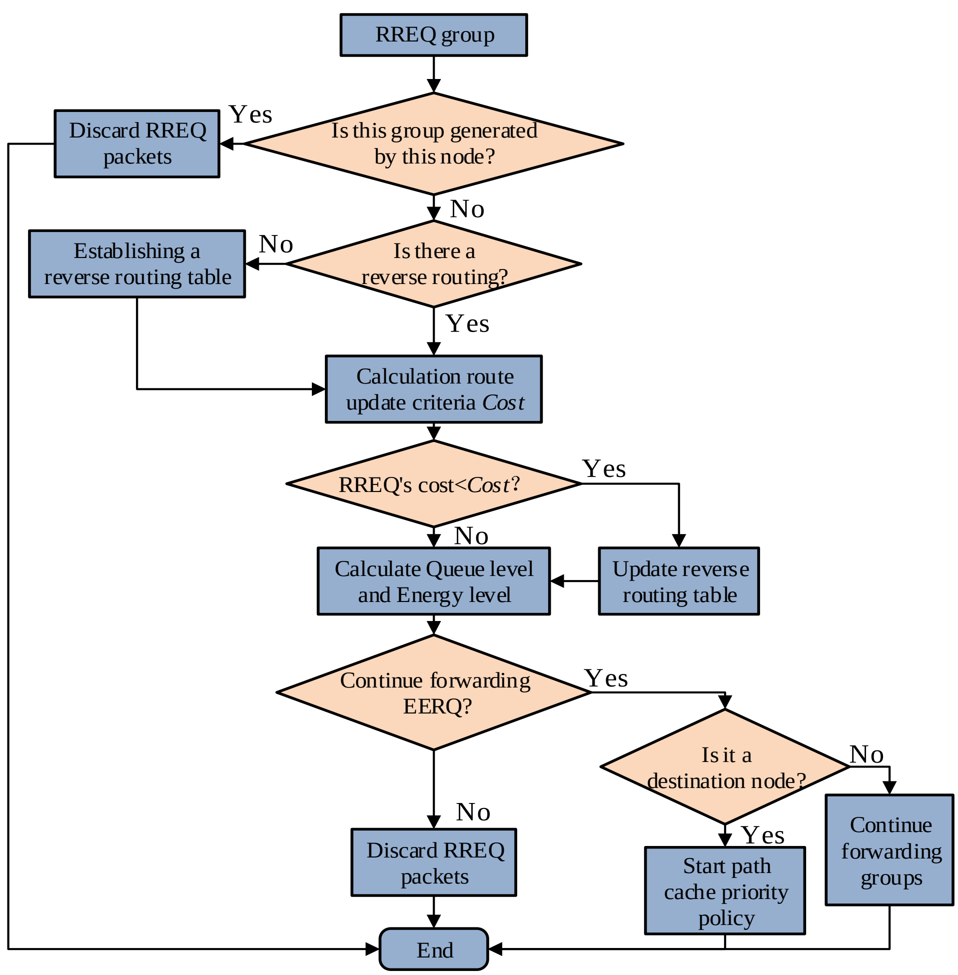

Figure 4. Flow chart of IMP-ZBR protocol processing RREQ.

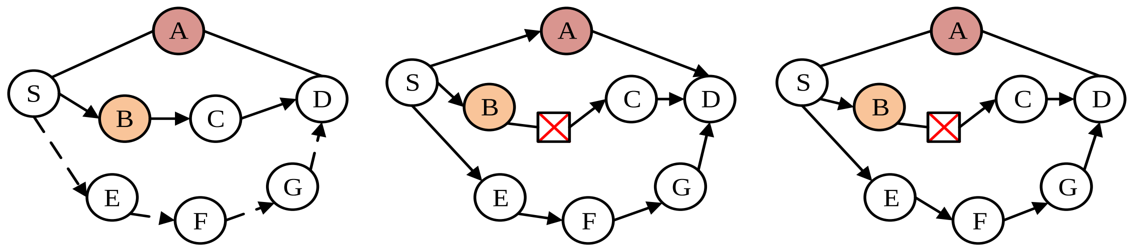

(a) Normal transmission (b) Node failure (c) Final result

Figure 5. IMP-ZBR algorithm for farmland data transmission.

The IMP-ZBR algorithm for the transmission of farm data was shown in Figure 5. The improved algorithm no longer adopted the principle of minimum number of hops in the path establishment process (Figure 5a). After comparing the *Cost* values of all possible paths, the primary path with the best overall performance as well as a backup path were finally established according to the prioritization rule.

Heterogeneous sensor data fusion based on improved evidence theory

In agricultural environmental DC systems, when there are multiple sensor nodes collecting specific kinds of data at the same moment, a large amount of redundant data is generated, and, if this information is transmitted directly to the end-user, it may reduce the communication efficiency and limit the effectiveness of the system due to wasted power. Therefore, data fusion algorithms were chosen for the study to generate the data required by the user after processing multiple redundant data. The correlation between the data fusion algorithm and the previously designed IMP-ZBR was that the former provided the latter with fused farmland data. Based on the types of sensors, data fusion methods can be categorized as isomorphic and heteromorphic, where Heterogeneous Data Fusion (HDF) is the difficulty. The study addressed the ambiguity and unknowns in multi-sensor data and designed an HDF method that combined cloud modeling and improved evidence theory. The fusion process of heterogeneous data was shown in Figure 6.

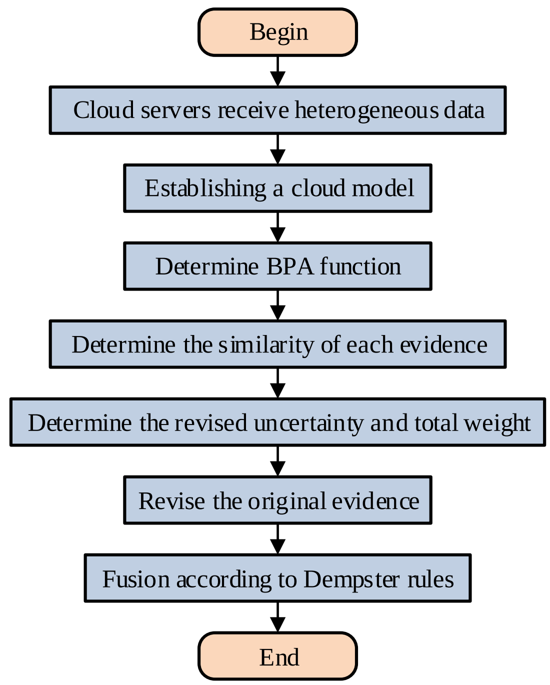

Figure 6. Flow chart of heterogeneous data fusion.

It is assumed that the data collected by several sensors deployed in the farmland are extracted after isomorphic data fusion and *n* heterogeneous data are generated and A body of evidence $X = (x_1, x_2, \cdots, x_n)$ is generated. Equation (4) illustrated how the cloud modeling theory determined the degree of affiliation between the discrete eigenvariable values.

$$u_{ij} = e^{-\frac{\left(x_i - E_{x_{ij}}\right)^2}{2E_{nij}'^{2}}} \tag{4}$$

where the affiliation of the i th class data corresponding to the j th evaluation index was represented by the u_{ij} in equation (4). The data expectation was denoted by $E_{x_{ij}}$, and the normal random number E'_{nij} was produced using super entropy as the standard deviation and $E_{x_{ij}}$ as the expectation. One of the most crucial factors in the cloud model is data super entropy, whose value is typically 0.01 and is established by professionals based on experience. The affiliation matrix $R_{n\times m}$ obtained based on the relevant numerical features and the cloud model basically satisfies the definition of the BPA function in the evidence theory, but does not satisfy the condition of $\sum_{j=1}^{m} u_{ij} = 1$ in the evidence theory. So, it needs to be reasonably transformed. The transformation of the affiliation degree was shown in Equation (5).

$$\begin{cases} \gamma_i = 1 - \max\left(u_{i1}, u_{i2},, u_{im}\right) \\ p_i\left(A_i\right) = \left(1-\gamma_i\right)\dfrac{u_{ij}}{\sum_{j=1}^{m} u_{ij}} \end{cases} \tag{5}$$

The value of the BPA function of the i th evidence related to the m th evaluation indication was represented by $p_i\left(A_i\right)$ in equation (5), whereas γ_i represented the uncertainty of the i th characteristic parameter. The quantity of assessment indicators was BBB. The matrix of BPA function was obtained as shown in equation (6).

$$P_{n\times(m+1)} = \begin{pmatrix} p_{11} & \cdots & p_{1m} & \gamma_1 \\ p_{21} & \cdots & p_{2m} & \gamma_2 \\ \vdots & \vdots & \vdots & \vdots \\ p_{n1} & \cdots & p_{nm} & \gamma_n \end{pmatrix} \tag{6}$$

The work enhanced the evidence theory based on similarity and certainty in an attempt to address the weaknesses of the conventional evidence theory in handling fusion conflict evidence. The relationship between each diverse piece of data was measured by the similarity of the evidence. The stronger the resemblance, the more reliable the evidence was, and as a result, it should be given more weight [19]. Currently, the conflict coefficient K, Jousselme distance, Pignistic probability distance, and cosine similarity are the classical measures used to describe the relationship between the evidence. However, a single relationship measure is not a good measure of the relationship between evidence. Therefore, this study proposed the fusion similarity. Equation (7) illustrated the local similarity s_{ij}, where $\Theta = A_1, A_2, \cdots, A_n$ was the identification framework definition.

$$\begin{cases} J\left(A_a, A_b\right) = \dfrac{\left|A_a \cap A_b\right|}{\left|A_a \cup A_b\right|}, \forall A_a, A_b \subseteq \Theta \\ s_{ij} = \left(1 - d_{BPA}\left(p_1, p_2\right)\right) \times \dfrac{\sum_{a=1}^{n}\sum_{b=1}^{n} p_i\left(A_a\right) p_j\left(A_b\right) \times J\left(A_a, A_b\right)}{\sqrt{\sum_{c=1}^{n} p_i\left(A_c\right)^2}\sqrt{\sum_{c=1}^{n} p_j\left(A_c\right)^2}} \end{cases} \tag{7}$$

where $J\left(A_a, A_b\right)$ was the Jaccard coefficient and $d_{BPA}\left(p_1, p_2\right)$ was the Jousselme distance between two pieces of evidence. Combined with the local similarity, the global similarity s_i of each piece of evidence could be derived, and the weight coefficient α_i based on similarity could be obtained by normalizing it as shown in equation (8).

$$\begin{cases} s_i = \sum_{j=1, i\neq j}^{n} s_{ij} \\ \alpha_i = s_i / \sum_{j=1}^{n} s_j \end{cases} \tag{8}$$

To determine the degree of certainty in the evidence and gauge its inherent qualities, the Hellinger distance was utilized in the study to quantify the separation between the intervals of certainty. Assuming that $R = \left\{r_1, r_2, \cdots, r_n\right\}$ and $T = \left\{t_1, t_2, \cdots, t_n\right\}$ were two probability distribution vectors of the random variable Z, their Hellinger distance $Hel\left(T|R\right)$ was shown in equation (9).

$$Hel\left(T|R\right) = \sqrt{\frac{1}{2}\sum_{i=1}^{n}\left(\sqrt{t_i} - \sqrt{r_i}\right)^2} \tag{9}$$

As the trust function defined as $Bel(g)$, the degree of confidence in the evidence supporting A_j was shown by $p_i(A_j)$, and the degree of certainty of the proposition was indicated by $Bel(p_i(A_j))$. Define $Bel(p_i(A_j))$ as the evidence's degree of confidence, it was determined by using the formula below.

$$DU(p_i)=\sum_{j=1}^{n}\sqrt{2}\times\sqrt{\left[\left(\sqrt{Bel(p_i(A_j))}-0\right)^2+\left(1-\sqrt{pl(p_i(A_j))}\right)^2\right]} \quad (10)$$

where $pl(p_i(A_j))$ was the likelihood function. The weight of evidence based on certainty was obtained after normalizing the evidence certainty, and the original evidence was corrected using the total weight of evidence. The certainty weight β_i was shown in equation (11).

$$\beta_i=\frac{DU(p_i)}{\sum_{j=1}^{n}DUp_j} \quad (11)$$

Finally, according to Dempster's rule, $n-1$ sub-fusion was performed on the weighted average processed body of evidence p. Dempster's combination rule was shown in equation (12).

$$p(A)=\begin{cases}\frac{1}{1-K}\sum_{B_i\cap C_j=A}p_1(B_i)p_2(C_j), A\neq\phi\\ 0, A=\phi\end{cases} \quad (12)$$

where B_i and C_j were the focal elements of the BPA function on the recognition framework. K was the conflict coefficient of evidence p_1 and p_2, which was calculated by equation (13).

$$K=\sum_{B_i\cap C_j=\phi}p_1(B_i)p_2(C_j) \quad (13)$$

Validation of IMP-ZBR protocol

In verifying the effectiveness of the IMP-ZBR protocol, The Network Simulator-ns-2 (https://www.isi.edu/nsnam/ns/) (NS2) simulation software was used to simulate and test this protocol as well as the NPZBR, RowBee, and ZBR protocols. The two key variables in the experimental setup were node pause time and CBR packet sending rate. The simulation experiment's parameters were configured as indicated in Table 1. Out of 50 nodes, 20 were selected to be responsible for specific tasks and remain stationary, and the remaining 30 nodes were set to move randomly. The simulation experiment scenarios were generated randomly by NS2 software, and the experimental results in a single scenario were contingent. Ten mobile scenarios were evaluated for each protocol under identical conditions to avoid this influence. The average of the findings was obtained to examine performance measures such as average end-to-end delay, packet delivery rate, route control expenditure, and route discovery frequency. In the first simulation scenario, this study modified the mobile nodes' stop times as 0, 50, 100, 150, 200, 250, and 300 seconds, respectively, and adjusted the CBR packet transmission rate to always be 2 packets/s. Node stop time has an impact on the network's topology change, as pause time increases, node mobility decreases, and the topology change also tends to stabilize gradually. In the second simulation scenario, the mobile node's stop time was adjusted to remain at 0 second, while the CBR packet sending rate was varied as 2, 4, 6, 8, 10, 12, 14, and 16 packets/s. The CBR packet sending rate indicated how much node loading was there in the network. The higher the sending rate, the more node loading was present and the higher the chance of congestion.

To show the efficacy of the improvement strategies suggested in this study, the data from the four common conflict kinds of the theory of evidence were combined, and the outcomes of comparable techniques for enhancing the theory of evidence were contrasted. The data used for testing was from Chengdu, Sichuan, China, and the calculation software used during the testing process was SPSS 22.0 (IBM, Armonk, New York, USA). The study chose three techniques to compare to confirm the efficacy of the data fusion algorithms, which included (1) using Jaccard coefficient to improve the cosine

Table 1. Simulation parameter settings.

No.	Parameter	Parameter value	No.	Parameter	Parameter value
1	Topology size	100 m × 100 m	1	Energy Model	Energy model
2	Nodes	50	2	Initial energy of nodes	60 J
3	Business type	CBR	3	Transmission power	0.69 W
4	Data grouping size	512 bytes	4	Received power	0.34 W
5	Simulation time	300 s	5	Sleep power	0.1 W

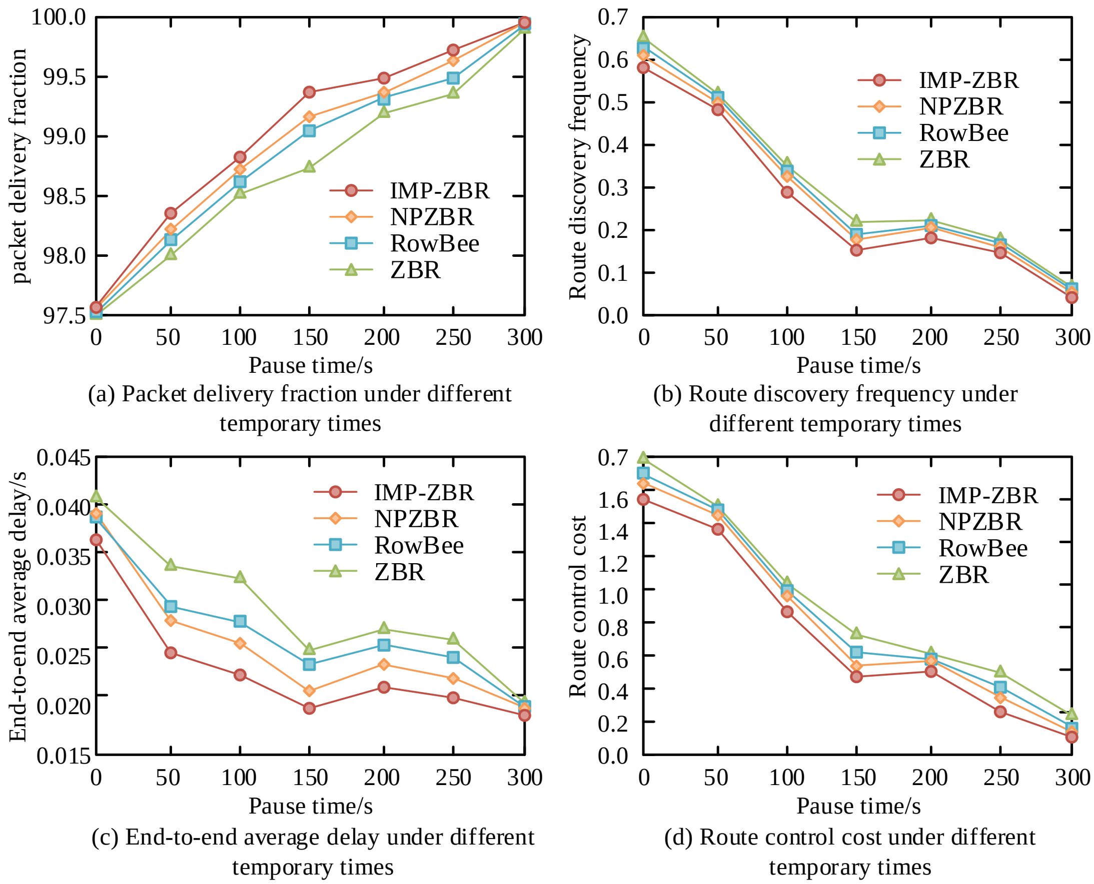

(a) Packet delivery fraction under different temporary times

(b) Route discovery frequency under different temporary times

(c) End-to-end average delay under different temporary times

(d) Route control cost under different temporary times

Figure 7. Simulation results under different pause times of mobile nodes.

similarity, thus obtaining the evidence similarity; (2) using Hellinger distance corresponding to the uncertainty intervals in the evidence to calculate the uncertainty of the evidence; (3) using cosine similarity to improve the conflict coefficient, thus defining the evidence conflict degree [20].

Results and discussion

The performance variations of the four routing algorithms

The performance variations of the four routing algorithms under various mobile node stop times were displayed in Figure 7. Although the packet delivery rates of the four routing protocols progressively approached one another after a pause time of 200 s, it was evident that the IMP-ZBR protocol's packet delivery rate was

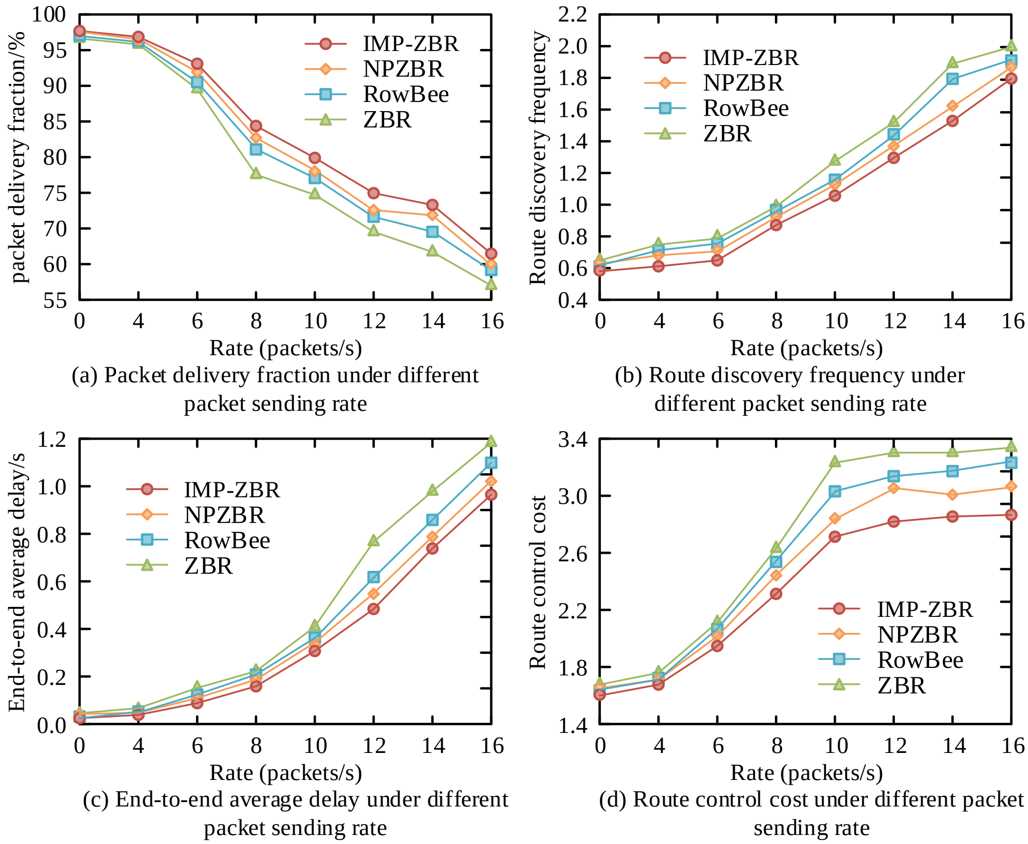

Figure 8. Simulation results under different packet sending rate.

consistently higher than the other three methods under various pause times (Figure 7a). The IMP-ZBR protocol always had lower route discovery frequency, average delay, and route control overhead than the other protocols (Figure 7b, c, and d). Congestion was significantly decreased by the IMP-ZBR protocol, which lowered the average delay of 2.4 ms, the route control overhead by 15%, and the frequency of route discovery by 15% when compared to ZBR. The variance of the four metrics for the four routing methods at various CBR packet sending speeds was shown in Figure 8. All the IMP-ZBR protocol's metrics were superior to those of competing protocols. The IMP-ZBR protocol significantly relieved congestion by lowering the average delay of 44 ms, the route control overhead by 12%, the route discovery frequency by 14%, and the packet delivery rate by an average of 4.5% when compared to the ZBR method. Through the simulation analysis, the study examined the impact of data fusion and validated the efficiency of the routing algorithm under varying mobile node pause times and CBR packet sending rates, which allowed for the analysis of farmland information based on improved ZigBee routing (IMP-ZBR) algorithms, as well as the effectiveness of DC. HDF validation studies were also carried out with real data to confirm the efficacy of the enhanced data fusion method.

Effectiveness of heterogeneous sensor data fusion based on improved evidence theory

The outcomes of the merging of BPA functions using various techniques were shown in Table 2. Although both the proposed method and the comparison method of the study gave correct results, the proposed method got a higher BPA function, which indicated better focus and higher confidence of the proposed method. To confirm the viability of the suggested data fusion technique, the study collected distinctive

Table 2. The fusion results from four common conflicts.

Algorithm	Conflict type	Proposition BPA				
		A	B	C	D	E
Jaccard-improved cosine similarity	Complete conflict	0.9996	0.0002	0.0002	/	/
	0 trust conflict	0.7628	0.2200	0.0172	/	/
	1 trust conflict	0.0006	0.0015	0.9980	/	/
	High conflict	0.9911	0.0025	0.0010	0.0000	0.0004
Hellinger Distance	Complete conflict	0.9792	0.0207	0.0001	/	/
	0 trust conflict	0.6510	0.2384	0.1106	/	/
	1 trust conflict	0.0273	0.0018	0.9709	/	/
	High conflict	0.9846	0.0040	0.0055	0.0001	0.0029
Improving conflict coefficients by cosine Similarity	Complete conflict	0.9994	0.0006	0.0000	/	/
	0 trust conflict	0.7560	0.1273	0.1167	/	/
	1 trust conflict	0.0001	0.0009	0.9990	/	/
	High conflict	0.9972	0.0010	0.0012	0.000	0.0005
This study	Complete conflict	0.9999*	0.0001	0.0000	/	/
	0 trust conflict	0.8436*	0.0418	0.1153	/	/
	1 trust conflict	0.0000	0.0006	0.9992*	/	/
	High conflict	0.9987*	0.0004	0.0006	0.0000	0.0003

Note: * represented the BPA maximum.

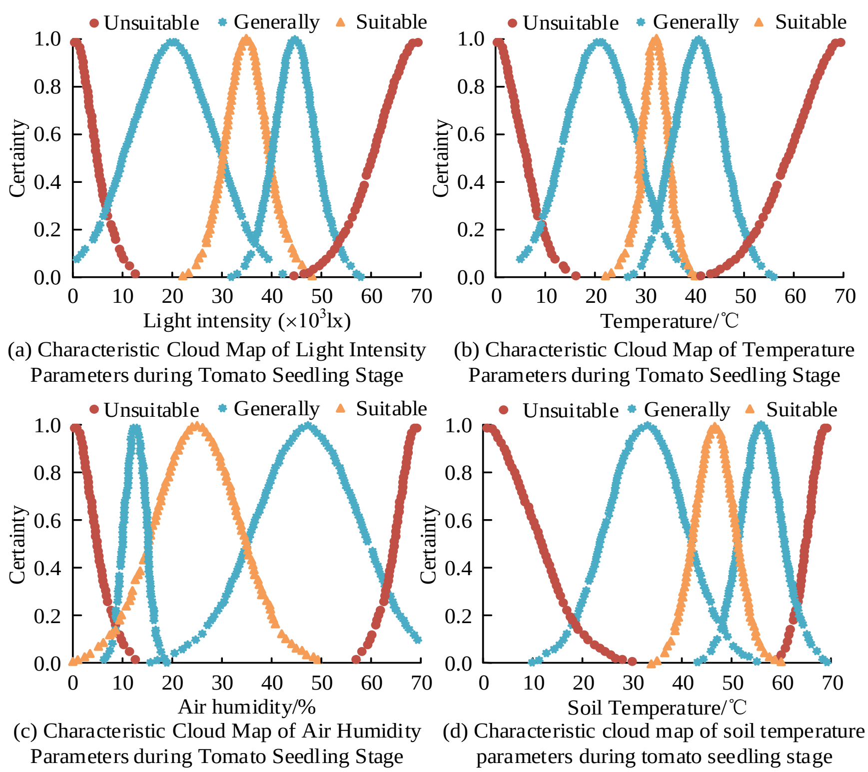

Figure 9. Cloud map of various characteristic parameters for tomato seedling growth.

characteristics impacting tomato development in wetlands and combined heterogeneous data.

Based on the evaluation indexes of each characteristic parameter, a cloud model was established for each characteristic parameter separately, and the evaluation results were categorized into suitable, general, and unsuitable groups (Figure 9). By fusing each characteristic parameter, the certainty of environment suitable, general, and unsuitable was obtained as 16.91%, 83.09%, and 0, respectively. According to the results of uncertainty, it could be concluded that the current growth environment of tomato was general, and it was necessary to regulate and observe the environment of tomato growth.

This study utilized ZigBee to establish a DC and analysis system for agricultural fields, addressing the possible issues of excessive node energy depletion and network congestion. Consequently, the IMP-ZBR protocol was proposed, which featured lower energy loss and a balanced load. The protocol had been enhanced to optimize the forwarding mechanism of intermediate nodes, update criterion for routing, and prioritization of cache paths. Additionally, considering the multi-sensor nature of DC applications, the study created an HDF method that used enhanced evidence theory and the cloud model to appropriately capture data uncertainty. The study findings indicated that implementing the IMP-ZBR protocol increased the packet delivery rate by an average of 4.5% compared to the ZBR algorithm across various CBR origination speeds. Moreover, the frequency of route discovery decreased by 14%, while the average delay and route control overhead were reduced by 44 ms and 12%, respectively. In the HDF validation experiments, the proposed method displayed outstanding focus and confidence, as seen in the remarkably high BPA function values. The results exhibited the excellent efficacy of the IMP-ZBR protocol in mitigating network congestion and enhancing algorithm functionality. The future research will intend to adopt additional metrics such as congestion and packet loss rate as routing state criteria to effectively mitigate network congestion and elevate overall network performance further.

References

1. Chinthamu N, Karukuri M. 2023. Data science and applications. Journal of Data Science and Intelligent Systems. 1(2):83–91.
2. Kumar P, Reddy SRN. 2020. Wireless sensor networks: A review of motes, wireless technologies, routing algorithms and static deployment strategies for agriculture applications. CSI Transactions on ICT. 8(3):331-345.
3. Bu F, Wang X. 2019. A smart agriculture IoT system based on deep reinforcement learning. Future Gener Comput Syst. 99:500-507.
4. Akhter R, Sofi SA. 2022. Precision agriculture using IoT data analytics and machine learning. Journal of King Saud University-Computer and Information Sciences. 34(8):5602-5618.
5. Feng X, Yan F, Liu X. 2019. Study of wireless communication technologies on Internet of Things for precision agriculture. Wirel Pers Commun. 108(3):1785-1802.
6. Muangprathub J, Boonnam N, Kajornkasirat S, Lekbangpong N, Wanichsombat A, Nillaor P. 2019. IoT and agriculture data analysis for smart farm. Comput Electron Agric. 156:467-474.
7. Sinha BB, Dhanalakshmi R. 2022. Recent advancements and challenges of Internet of Things in smart agriculture: A survey. Future Gener Comput Syst. 126:169-184.
8. Gao X, Zhang T, Xie W, Chen B, Chen S. 2019. A node-protection-based ZBR routing algorithm. IEEE Access. 7:180064-180072.
9. Heidari E, Movaghar A, Motameni H, Barzegar B. 2022. Reducing energy consumption in IoT by a routing whale optimization algorithm. Malaysian J Comput Sci. 35(2):142-157.
10. Gao D, Zhang S, Zhang F, He T, Zhang J. 2019. RowBee: A routing protocol based on cross-technology communication for energy-harvesting wireless sensor networks. IEEE Access. 7:40663-40673.
11. Bodunde OP, Adie UC, Ikumapayi OM, Akinyoola JO, Aderoba AA. 2019. Architectural design and performance evaluation of a ZigBee technology based adaptive sprinkler irrigation robot. Comput Electron Agric. 160:168-178.
12. Chi Z, Li Y, Sun H, Haung Z, Zhu T. 2021. Simultaneous bi-directional communications and data forwarding using a single ZigBee data stream. IEEE ACM Trans Netw. 29(2): 821-833.
13. Pilger N, Berg A, Joosse P. 2020. Semi-automated roadside image data collection for characterization of agricultural land management practices. Remote Sens. 12(14):2342-2353.
14. Lin C, Han G, Qi X, Du J, Xu T, Miguel MG. 2021. Energy-optimal data collection for unmanned aerial vehicle-aided industrial wireless sensor network-based agricultural monitoring system: A clustering compressed sampling approach. IEEE Trans Industr Inform. 17(6):4411-4420.
15. Stoll GP, Luck JD, Pitla SK, Rohrer RA. 2021. Integration of auxiliary sensor data to isobus for agricultural machinery data collection. Appl Eng Agric. 37(1):157-162.
16. Xiao F. 2019. Multi-sensor data fusion based on the belief divergence measure of evidences and the belief entropy. Inf Fusion. 46:23-32.

17. Lin T, Wu P, Gao F. 2022. Information security of flowmeter communication network based on multi-sensor data fusion. Energy Rep. 8:12643-12652.
18. Komilov DR. 2023. Application of Zigbee technology in IOT. International Journal of Advance Scientific Research. 3(09):343-349.
19. Luo N, Yu H, You Z, Li Y, Zhou T, Jiao Y, *et al*. 2023. Fuzzy logic and neural network-based risk assessment model for import and export enterprises: A review. Journal of Data Science and Intelligent Systems. 1(1):2-11.
20. Li J, Xie B, Jin Y, Hu Z, Zhou L. 2020. Weighted conflict evidence combination method based on Hellinger distance and the belief entropy. IEEE Access. 8:225507-225521.